The Thesis Committee for Spencer Austin Kerns
Certifies that this is the approved version of the following thesis:

Synthesis and Metallation of a Novel Anthracene Ligand Architecture for Development of Structural Models of Mono [Fe]-hydrogenase

APPROVED BY
SUPERVISING COMMITTEE:

Supervisor:

Michael J. Rose

Emily Que

Synthesis and Metallation of a Novel Anthracene Ligand Architecture for Development of Structural Models of Mono [Fe]-hydrogenase

by

Spencer Austin Kerns, B.A.

Thesis

Presented to the Faculty of the Graduate School of

The University of Texas at Austin

in Partial Fulfillment

of the Requirements

for the Degree of

Master of Arts

The University of Texas at Austin

December 2016

Acknowledgements

I would like to thank those who have guided and supported me through these two years of graduate school at The University of Texas at Austin: namely, the professors for their instruction in both academic courses and research endeavors; Dr. Michael Rose for his daily guidance, patience, and understanding in this process; my fellow group members, especially those in the Hydrogenase subgroup, for their thoughtful discussions and their contributions to making each day in lab enjoyable; Pisey Vong and Anne-Clarisse Magtaan for their help in ligand synthesis; and my family, for their unbridled support through this process and constant comfort.

Abstract

Synthesis and Metallation of a Novel Anthracene Ligand Architecture for Development of Structural Models of Mono [Fe]-hydrogenase

Spencer Austin Kerns, M.A.

The University of Texas at Austin, 2016

Supervisor: Michael J. Rose

Herein reported is the design and synthesis of a novel ligand architecture for the development of synthetic model complexes of mono [Fe]-hydrogenase. The ligand utilizes a functionalized anthracene scaffold that spatially directs *fac*-coordination of the $C^{NH}N^{py}S^{thiol}$ donors characteristic of the active site. Metallation of the ligand was performed with $[Fe(CO)_4Br_2]$ in the absence and presence of various bases in order to develop iron dicarbonyl complexes of relevance to the active site of mono [Fe]-hydrogenase. The choice of base serves an important role in mediating reactivity and affords different complexes as evidenced by IR spectroscopy.

Table of Contents

I. INTRODUCTION

The dihydrogen (H_2) metabolism performed by the family of hydrogenase enzymes is a key process in energy utilization in certain microorganisms. There are presently three identified classes of hydrogenase enzymes that exist in Nature: [Fe-Fe] hydrogenase, [Ni-Fe] hydrogenase, and mono [Fe]-hydrogenase. The hydrogenase enzymes are phylogenetically distinct, but share a unique set of non-proteinaceous ligands that do not occur in other metalloenzymes. These carbon monoxide or cyanide ligands represent a converged structural trait that likely facilitates the related catalytic reactivities of the hydrogenase enzymes.

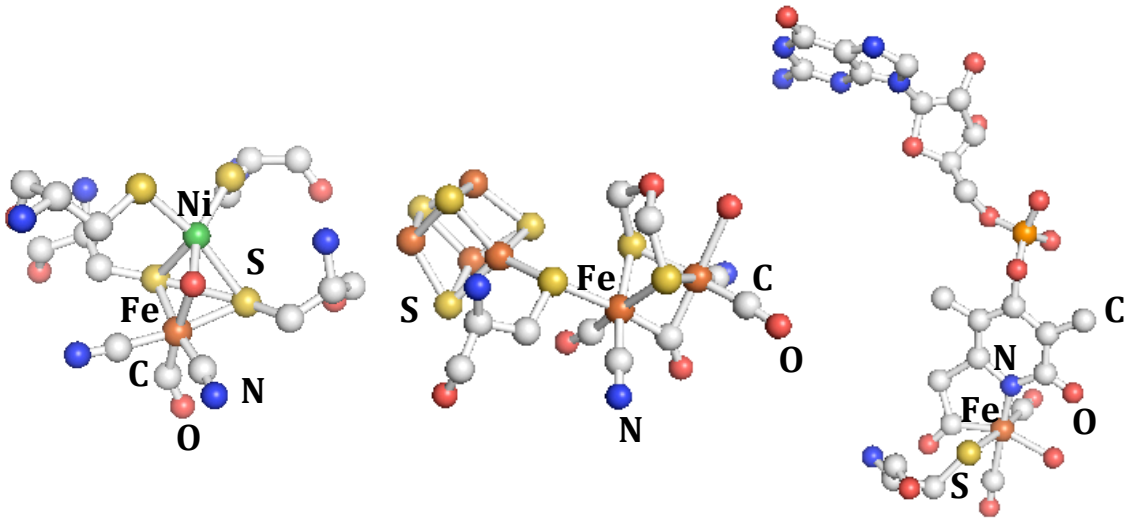

Figure 1: The three classes of hydrogenases - [Ni-Fe] hydrogenase[1a] (left), [Fe-Fe] hydrogenase[1b] (center), and mono -[Fe]-hydrogenase[1c] (right).

The dinuclear [Fe-Fe] and [Ni-Fe]-hydrogenases catalyze the reversible oxidation of dihydrogen or $H_2 \rightleftharpoons 2H^+ + 2e^-$. This redox reaction serves to couple the oxidation of H_2 with energy liberating processes or reduce protons in order to reuse oxidized electron carriers. Mono [Fe]-hydrogenase, also known as H_2-forming

methylenetetrahydromethanopterin (Hmd), exhibits unique reactivity in that the metal center is not redox-active, instead catalyzing the heterolytic cleavage of dihydrogen or $H_2 \rightleftharpoons H^+ + H^-$. Additionally, the enzyme exhibits substrate dependence, resulting in hydride transfer to methenyltetrahydromethanopterin (methenyl-H_4MPT^+), which is an intermediate step in the conversion of CO_2 to methane in methanogenic archaea under nickl-limited conditions.

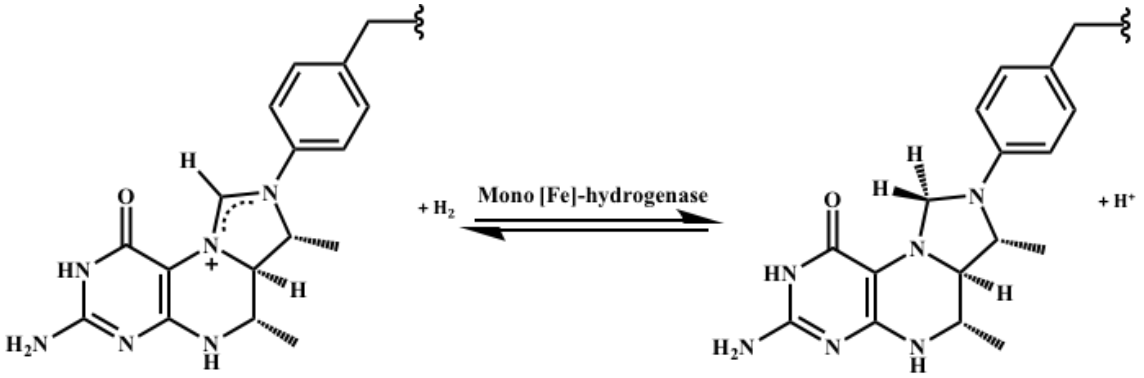

Figure 2: The reduction of methenyltetrahydromethanopterin (methenyl-H_4MPT^+) to methylenetetrahydromethanopterin (methylene-H_4MPT) as performed by mono [Fe]-hydrogenase.

The consumption and production of H_2 performed by the hydrogenase enzymes has inspired an increasing interest in these enzymes as affordable catalysts for sustainable and clean energy. The dynamic and reversible conversion of H_2 to protons and electrons demonstrated by the [Fe-Fe] and [Ni-Fe] hydrogenases encouraged research into the structural and mechanistic aspects of these enzymes, and their viability as electrocatalysts in the development of a hydrogen economy. In contrast, the reactivity of mono [Fe]-hydrogenase has been studied less extensively, prompting the need for further structural and mechanistic studies in the development of more affordable industrial catalysts.

Mono [Fe]-hydrogenase was originally believed to be a metal-free enzyme until Thauer and coworkers reported the presence of an iron cofactor in 2004.[2] Early characterization of mono [Fe]-hydrogenase relied on data obtained by IR,[3] EXAFS,[4] and Mössbauer spectroscopies.[5] IR and EXAFS studies demonstrated the presence of two *cis* carbonyl ligands in the active site, revealing the conserved nature of the carbonyl ligand amongst the three hydrogenases. EXAFS data additionally suggested that a four or five-coordinate low-valent Fe center was present in the active site; this was later supported by Mössbauer spectroscopy, which confirmed that the metal center is Fe(II).[6]

The first crystal structure of mono [Fe]-hydrogenase was published in 2008 by Shima, *et. al.*[7] The crystal structure was originally interpreted to contain a pyridinol moiety with a pendant carboxylic acid as pictured in A of Figure 3. However, further diffraction studies revealed steric hindrances associated with this model. In 2009, a refined structure B (Figure 3) revealed that the enzyme active site consists of an octahedrally coordinated Fe(II) metal center, chelated by the N and C donors of a unique acylmethylpyridone moiety in a facial arrangement with the sulfur of Cys176, the only proteinaceous ligand.[8] The orthogonal face of the active site consists of two *cis*-

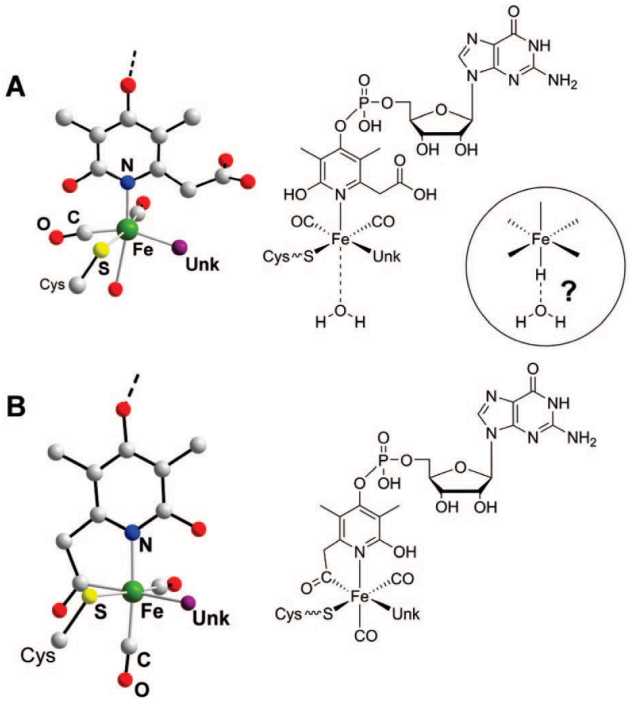

Figure 3: A comparison of the original structure (A) and revised structure (B) of the mono-[Fe] hydrogenase enzyme active site. Figure is taken from reference 9.

coordinated carbonyl ligands and a weakly bound solvent site, typically attributed to water. Synthetic models of mono [Fe]-hydrogenase have since rapidly progressed, incorporating three important aspects of the enzyme active site in various combinations and to varying extents: the organometallic iron-acyl bond, *fac* coordination of the carbon, nitrogen, and sulfur donors, and a thiolate sulfur donor mimicking the cysteine residue.

Hu and coworkers first accessed acyl-containing analogues through the reaction of the anionic, acyl-containing iron precursor **1** with sodium 2-mercapto-6-methylpyridine.[9] This reaction resulted in the dimerized product **2** containing bridging thiolate ligands. Monomeric units were isolated via introduction of an array of ligands generating **3a-d**. While complexes **3c** and **3d** contain no abiological ligands, the acyl unit remains unincorporated into a chelating system, and the thiolate sulfur donor is incorporated in a substituted pyridine moiety featuring an unfavorable four-membered chelating ring – uncharacteristic of the active site.

Scheme 1: Synthetic route demonstrating the first example of acyl ligation incorporated in a synthetic model of mono [Fe]-hydrogenase by Hu and coworkers.

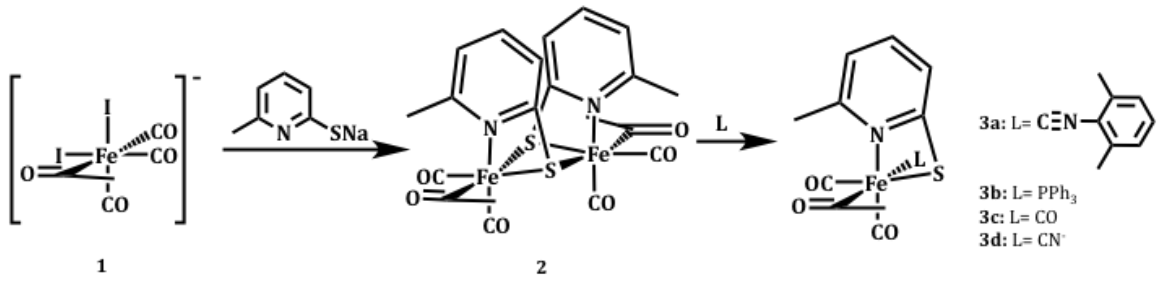

1 2

Complexes containing the acylmethylpyridine chelating motif were achieved by treatment of a substituted 2-methylpyridine moiety with *n*-butyllithium at 0 °C followed by reaction with $Fe(CO)_5$ at –50 °C to generate intermediates **4a** or **4b**.[10] Oxidation of **4a** and **4b** by I_2 generated the tricarbonyl complexes **5a** and **5b**, which were reacted with sodium 2-mercapto-6-methylpyridine to synthesize the final products **6a** and **6b** (Scheme 2). Crystallographic data was in accordance with typical bond lengths for Fe(II)-acyl-thiolate complexes and revealed the preferred position of the anionic thiolate donor *trans* to a carbonyl ligand, rather than the anionic acyl ligand. The IR spectra of **6a** and **6b** exhibited *v*(CO) stretches at 2029 and 1962 cm^{-1} and 2026 and 1961 cm^{-1}, respectively, in comparison to the those of the enzyme at 2011 and 1942 cm^{-1}. Both complexes failed to react with dihydrogen, likely attributable to the incorporation of the chelating pyridine-thiolate moiety and absence of an open coordination site.

Scheme 2: Synthetic routes employed by Hu and coworkers in the development of synthetic models of mono [Fe]-hydrogenase.

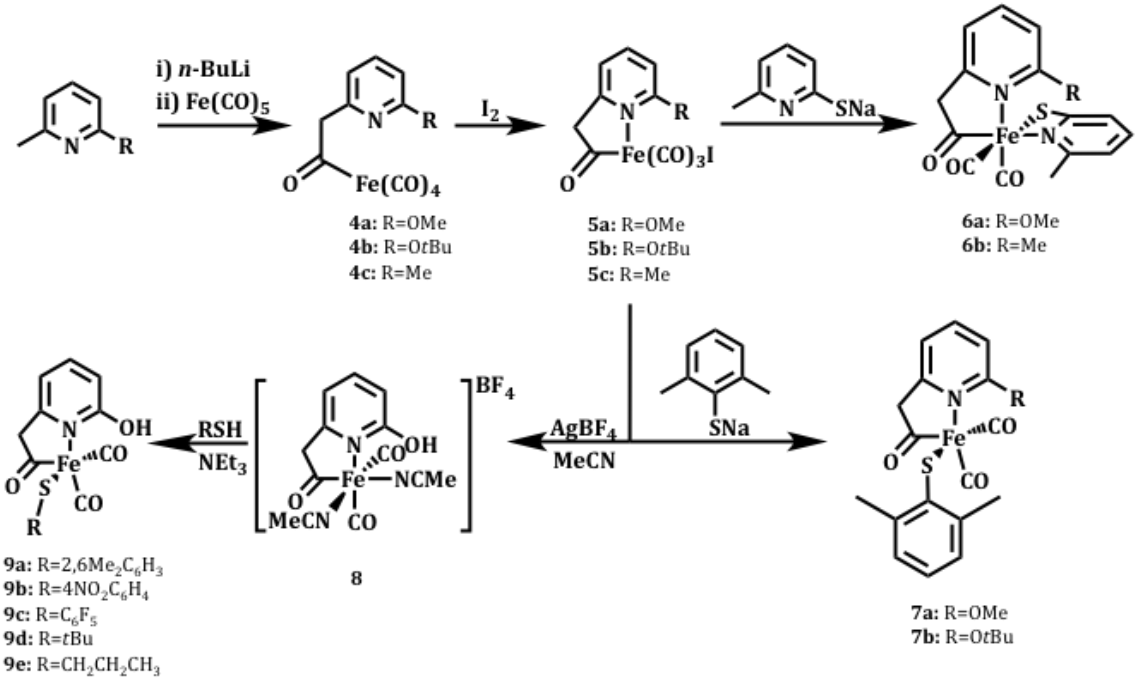

Hu and coworkers applied the previously described methods to synthesize a five-coordinate acylmethylpyridine complex. The tricarbonyl complexes **5a,b** were reacted with sodium 2,6-dimethylbenzenethiolate affording **7a,b**.[12] The site *trans* to the acyl ligand is unoccupied, exhibiting the stronger *trans*-influence of the organometallic iron-acyl bond in comparison to CO. Notably, complexes **7a** or **7b** did not react with H_2, prompting the synthesis of acylmethylpyridinol complexes, which better mimic the secondary coordination sphere of the enzyme active site. Attempts at direct deprotection of **7b** were unsuccessful.[13] Instead, **5b** was treated with Me_3Si and H_2O in order to deprotect the *t*Bu group to generate acylmethylpyridinol moiety.[14] The solvent bound complex **8** was used to synthesize a series of thiolate-bound acylmethylpyridinol complexes **9a-e**. These complexes exhibit low stability, demonstrating both light and temperature sensitivity. Complex **9c**, the only viable complex with a lifetime enabling

catalytic studies, however, did not demonstrate reactivity with H_2 as monitored by ^1H NMR.

Pickett and coworkers concurrently developed a synthetic route accessing the organometallic carbon-iron bond through a five-membered carbamoyl ring system.[11] In this synthetically facile method, reaction between $[Fe(CO)_4Br_2]$ and 2-aminopyridine results in nucleophilic attack of one of the carbonyl ligands and the product **10** containing a ferracyclic ring that closely resembles that of the enzyme active site. Complex **10** was treated with 2-mercaptoethanol to emulate the ligand donors of the natural system. The crystallized product **11** was a dimerized species containing bridging thiolate ligands as seen previously in **2**.

Scheme 3: Synthetic route employed by Pickett to introduce the carbamoyl ligation motif in synthetic models of mono [Fe]-hydrogenase.

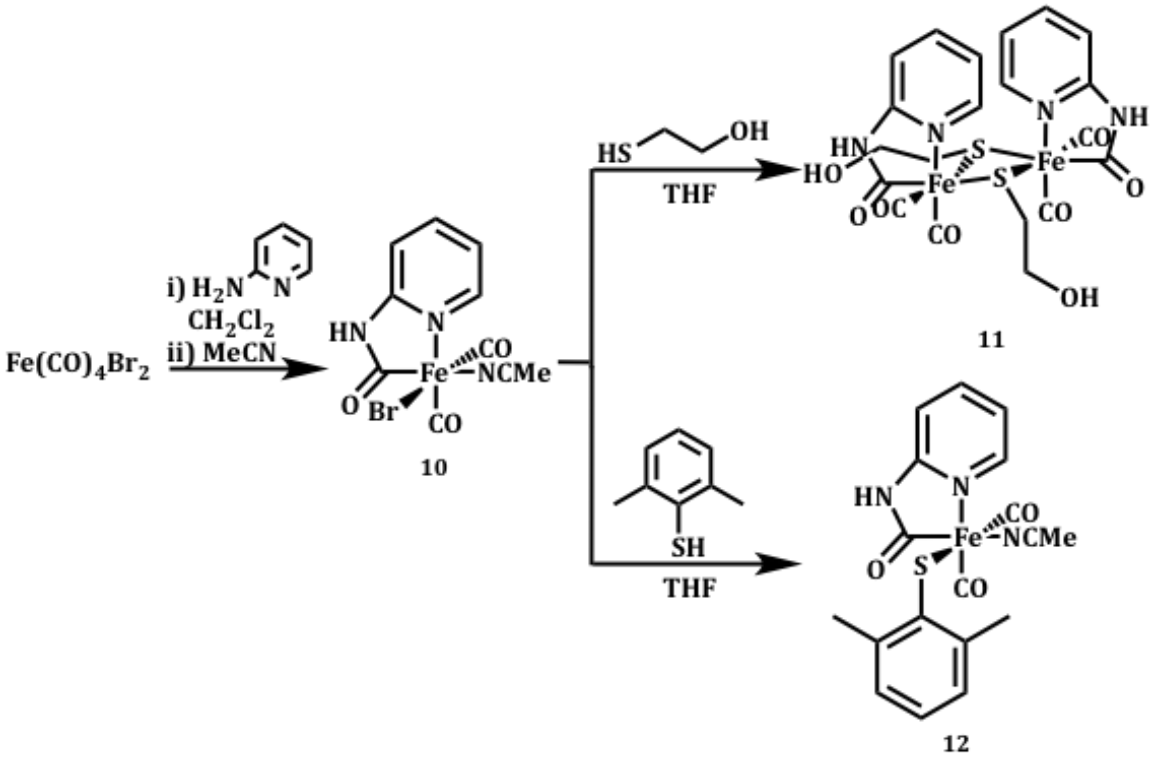

Instead, complex **10** was then treated with 2,6-dimethylbenzenethiol in order to avoid the formation of the dimerized species, resulting in the synthesis of **12**. Complex **12** presents no significant structural deviation in comparison to the primary coordination sphere of the natural system as shown in Figure 3 (B). The chelating ligand of **12** exhibits both a similar bite angle and similar bond distances in comparison to the enzyme active site, while the *cis*-coordinated CO ligands are both bound at slightly shorter bond distances. The isolated product **12** exhibits *cis* carbonyl stretches at 1958 and 2026 cm^{-1} in the IR spectrum that closely approximate those found in the natural system (in water) at 1972 and 2031 cm^{-1}. The increased difference in CO stretch frequency in comparison

to the enzyme may be attributable to electronic differences imposed by the carbamoyl unit in comparison to the naturally occurring acyl unit.

Song and coworkers have also devised a unique synthetic route in the development of acyl-containing models of mono [Fe]-hydrogenase. A substituted pyridine moiety is reacted with Collman's reagent, resulting in nucleophilic substitution and the unstable intermediate **13**.[15] In-situ CO migratory insertion results in the synthesis of the acyl unit and coordination of the methylhydroxy group occurs as **13** is oxidized with I_2 or Br_2, generating **14**. Finally, **14** is treated with a thiolate salt in order to remove the bound halide affording complexes **15a-e**. Interestingly, both the acylmethylpyridyl and the hydroxymethylpyridyl moieties form five-membered ferracyclic rings, with the weakly bound hydroxyl group serving as an approximation of the bound H_2O ligand and a structural approximation of the hydroxyl group in the enzyme active site.

Song and coworkers later synthesized **16a**, the first example of a crystallographically characterized synthetic model of mono [Fe]-hydrogenase bearing an acylmethylpyridinol ligand.[16] In **16a,b**, the thiolate sulfur donor is incorporated in a bidentate 2-mercaptoacyl-6-methoxypyridine ligand, reminiscent of those utilized by Hu and coworkers in **6a** and **6b**. However, the bound pyridine moiety *trans* to the acyl unit precludes any reactivity with H_2 by occupying the solvato–site in these models.

Scheme 4: Synthetic route employed by Song and coworkers to incorporate a methylhydroxy group in models of mono [Fe]-hydrogenase.

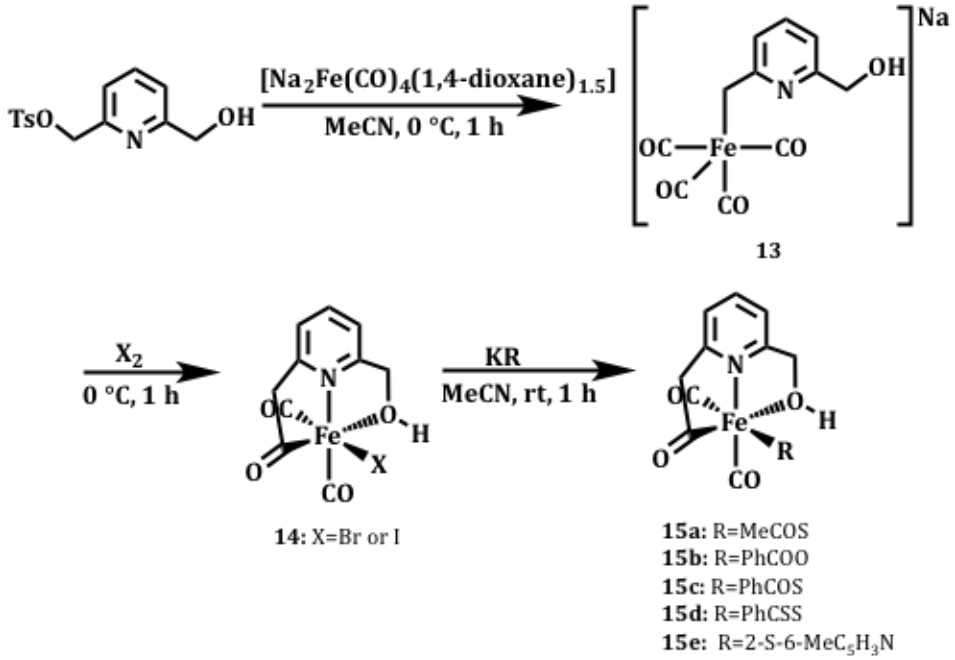

Scheme 5: Synthetic route employed by Song and coworkers to incorporate an acylmethylpyridinol moiety in a structurally characterized model of mono [Fe]-hydrogenase.

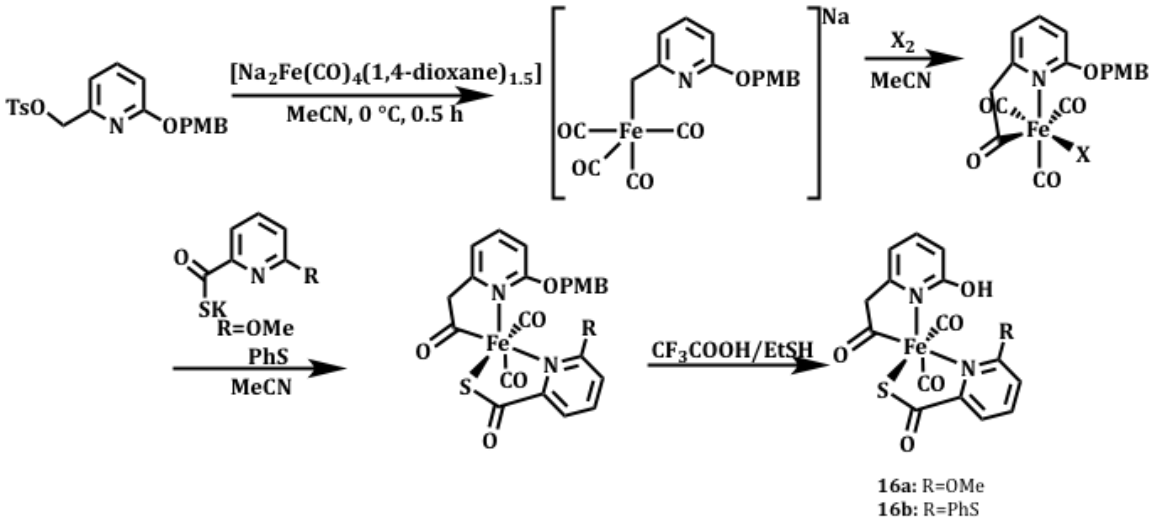

The mono [Fe]-hydrogenase models synthesized by the Hu, Pickett, and Song groups serve as mostly accurate structural mimics of the enzyme active site; however, these models have not been shown to activate dihydrogen. Many of the current models lack an open coordination site, preventing the binding and subsequent activation of H_2 across the metal center, viz a vis formation of a metal hydride species. The five-coordinate complexes such as **9a-e** that have been synthesized are not robust, lacking stability at ambient conditions, and are limited in both the scope of allowed experiments and their means of detection necessary for catalytic studies and the detection of potential iron-hydride intermediates related to the enzyme's activity.

SCOPE OF THIS WORK

One area of improving the present dearth of structural/functional models of this enzyme includes 'molecular scaffolding.' This process imparts controlled spatial arrangement of donor ligands in the design and synthesis of metal complexes. As a result, both the final geometry of the complex and the binding affinity of the ligands may be modulated by the molecular scaffold. The rigid structure of substituted anthracene scaffolds has been utilized in both *trans*-spanning[18,19] and *cis*-chelating[20] ligand architectures. In this work, a substituted 1,8-anthracene backbone is employed as a molecular scaffold for the construction of synthetic models of mono [Fe]-hydrogenase. Meta-substitution of the coupled phenyl units enables *cis*-chelation of nitrogen and sulfur donor ligands, ultimately promoting the facial-coordination of the N,C,S binding moieties characteristic of the enzyme active site as demonstrated in Figure 4. Additionally, the anthracene scaffold enables tethering of the C, N, and S donor atoms, which may impart further stability to the final metal complex via the chelate effect and combat difficulties associated with the synthesis and isolation of $L_xM(H)(SR)$ type complexes. For example,

protonation of the thiolate moiety often results in labile thiol ligands and there exists a competing tendency to eliminate H_2 in a binuclear reaction or reductively eliminate RSH from a mononuclear metal center. Overall, the resulting system should facilitate catalytic studies through the potential for dynamic S binding/unbinding and increased stability, aiding in the detection of important intermediates (i.e. iron hydride complexes).

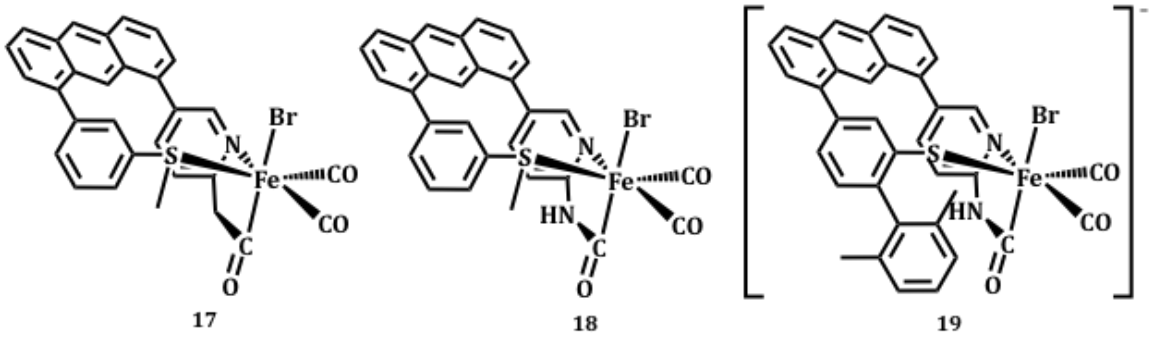

Figure 4: A schematic representation of thioether and thiolate containing synthetic models of mono [Fe] hydrogenase utilizing an anthracene backbone.

Transition metal thiolate hydride complexes resembling possible intermediates of the mono [Fe]-hydrogenase active site have been successfully synthesized by oxidative addition of thiols across the an unsaturated ruthenium center or by hydride/thiolate exchange reactions between metal dihydrides and disulfides.[21,22] However, due to the decreased electron density of iron, synthetic routes relying on oxidative addition are not feasible. Darensbourg and coworkers developed an elegant synthetic route utilizing anionic iron thiolate complexes of varying (-SR) groups to control the site of protonation (iron center or thiolate sulfur) on the basis of the electron density of the thiolate ligand.[23,24] Using this method, these researchers prepared the first iron thiolate-hydride complex $(PhS)Fe(H)(CO)_2(P(OPh)_3)_2$ structurally characterized by X-ray crystallography.[25] Such complexes still remain rare, with only nine other structurally

characterized iron thiolate-hydride complexes[26-32] and a single iron thioether-hydride complex[33] in existence.

The scarcity of iron thioether-hydride complexes in existence may reveal the importance of the cysteinyl sulfur in the mono [Fe]-hydrogenase active site. In biology, cysteine maintains a variety of functions including – but not limited to – structural stabilization, catalysis, redox-signaling, and metal-binding due to the flexible redox properties of sulfur. With respect to mono [Fe]-hydrogenase, the cysteine moiety likely functions to anchor the enzyme active site in the proper position to encounter the substrate. Additionally, computational studies[34] have suggested that the cysteinyl sulfur may act as a viable proton acceptor in the activation of H_2, analogous to that proposed by Lubitz and coworkers in the [Ni-Fe] hydrogenase.[35]

The role of the nucleophilic thiolate sulfur in model complex **19** (see Figure 4) will be investigated by comparison to structurally related and spectroscopically characterized thioether-containing complexes, **17** and **18**. Following halide abstraction, both **17** and **18** were shown to generate Fe–H species upon reaction with H_2 in the presence of base as evidenced by ^{1}H NMR resonances. However, these complexes were not shown to demonstrate hydride transfer reactivity to organic substrates without decomposition, possibly due to decreased electron density at the metal center when compared to the enzyme active site. In both **17** and **18**, the active complexes for hydride transfer are neutral, in contrast to the formally anionic complex active in nature. It can then reasonably be inferred that the substitution of an anionic thiolate ligand (such as that proposed in **19**) in place of the thioether moieties will promote the transfer of a hydride, in accordance with previous notions of thermodynamic hydricities of transition metal complexes.[36]

II. Results and Discussion

A bulky, biphenyl thioether moiety was first synthesized according to Scheme 6. The resulting synthon **20** contains an appended *meta*-xylene in the position para to the bromo site in order to prevent dimerization of products that may result upon conversion of the thioether moiety into a thiol prior to metallation.

Scheme 6: Synthetic route[a] for preparation of the bulky, biphenyl thioether moiety.

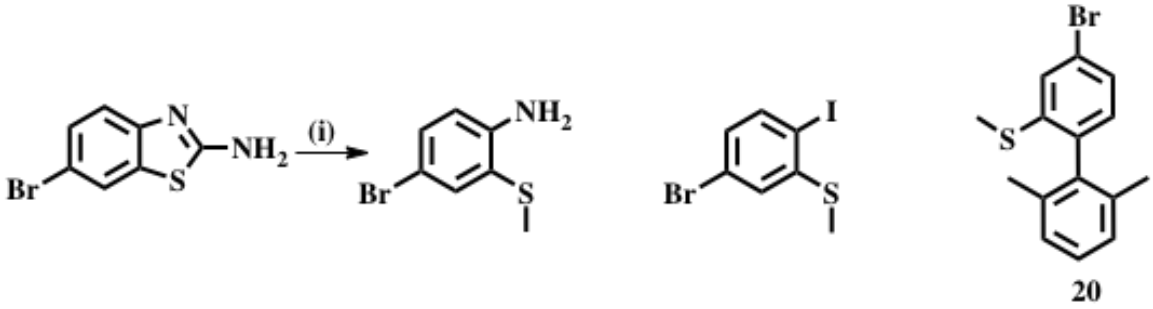

20

[a](i) KOH (aq) reflux, MeI (isolated yield 89%) (ii) HCl, $NaNO_2$ (aq), NaI (aq), acetone (isolated yield 79%) (iii) $Ba(OH)_2 \bullet 8H_2O$, 2,6-dimethylphenylboronic acid, $[Pd(PPh_3)_4]$, dioxane/H_2O (3:1) (isolated yield 88%).

Then, a 1,8-dichloroanthracene backbone was asymmetrically functionalized by subsequent Suzuki couplings of 2-amino-5-bromopyridine and the bulky, biphenyl thioether moiety **20** to generate ligand **21** (Scheme 7). The anthracene scaffold provides a rigid framework that enables the tethering of the three C,N,S donor atoms in a single asymmetric ligand which may impart further stability to the final metal complex and more sustained catalytic activity as described by Rose and coworkers.[37]

Scheme 7: Synthetic route[a] for substituted anthracene backbone for metallation.

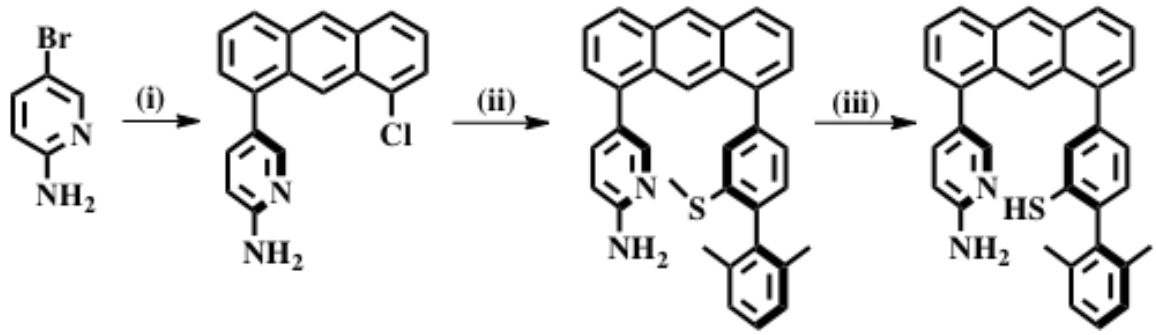

21 22

[a](i) KOAc, B_2pin_2, Pd_2dba_3/SPHOS, K_3PO_4, 1,8-dichloroanthracene, dioxane/H_2O (isolated yield 38%) (ii) KOAc, B_2pin_2, Pd_2dba_3/SPHOS, K_3PO_4, (4-Bromo-2',6'-dimethyl-[1,1'-biphenyl]-2-yl)(methyl)sulfane, dioxane/H_2O (isolated yield 81%) (iii) NaH, ^{t}nonyl-mercaptan, HCl (aq), DMF (isolated yield 46%).

Initial attempts at coupling to the anthracene backbone relied on conversion of synthons 2-amino-5-bromopyridine and **20** into the boronic acid congeners. However, isolation of the boronic acid congener of **20** proved inconsistent and did not result in coupling to the anthracene backbone via simple [$Pd(PPh_3)_4$] catalyzed Suzuki couplings or Negishi coupling reactions. Instead, 2-amino-5-bromopyridine was first coupled to the 1,8-dichloroanthracene backbone by in situ generation of the boronic ester congener and subsequent aqueous conversion to the boronic acid in the presence of a [$Pd_2(dba)_3$]/SPHOS catalyst system affording the mono-substituted, asymmetric product in low yield. Rose and coworkers previously outlined the importance of the biaryl phosphine co-catalyst in mediating the substitution of the anthracene backbone with respect to the coupling of pyridine and thioether substituents in which SPHOS generated

a less active PdL_1 species that enabled asymmetric coupling.[38] Further addition of **20** to the anthracene scaffold was achieved in a similar fashion with a $[Pd_2(dba)_3]$/XPHOS catalyst system. Notably, oxidative addition of **20** and conversion to the boronic ester intermediate proceeded much more slowly, presumably due to the increased bulk of the substrate around the Pd center during transmetallation. Following complete functionalization of the anthracene scaffold to **21**, the thioether moiety was subsequently deprotected by generation of the sodium salt in the presence of *tert*-nonyl mercaptan and protonation by addition of 3 M HCl to generate **22**.

Initial complexation of **22** with $[Fe(CO)_4Br_2]$ was performed under air-free, dark conditions at –40 °C, stirred for 15 minutes, and warmed to room temperature. The resulting solution was filtered and precipitated from diethyl ether to yield a sand-yellow powder. The resulting species was proposed to be a charged dicarbonyl species or neutral piano-stool type complex with three carbonyls, depending on the generation of one or two equivalents of HBr as a reaction byproduct, respectively. Carbonyl stretches were observed at 2095 and 2042 cm^{-1} and an additional feature at 1613 cm^{-1}, attributed to the (C=O) bond of the carbamoyl unit. While the frequencies of the two carbonyls are consistent with *cis*-arrangement, the carbonyl stretches occur at higher frequencies than those of other thiolate-bound and thiother-bound synthetic models previously mentioned.

Metallation of **22** with $[Fe(CO)_4Br_2]$ was also performed in the presence of differing acetate bases, KOAc and $(NEt_4)(OAc)$. Metallation in the presence of one equivalent of potassium acetate yields a product that was virtually indistinguishable by IR analysis, yielding carbonyl stretches at 2096 and 2040 cm^{-1}. Likely, the low solubility of the base in the organic solvent disallows any role in deprotonation of the anthracene ligand, resulting in a similar product to the reaction performed in the absence of base. Complexation was then performed in the presence of organic acetate bases to achieve

greater solubility. Addition of $(NEt_4)(OAc)$ to **22** resulted in a rapid color change from yellow-orange to red-orange. Complexation with $[Fe(CO)_4Br_2]$ under similar conditions yielded a product with multiple carbonyl stretches. The product exhibited greater solubility, enabling purification by alumina column. Concentration of the fraction eluted with DCM yielded a yellow-orange powder with ν(CO) features at 2025 and 1962 cm^{-1} and a similar carbamoyl stretch at 1614 cm^{-1}. The carbonyl stretches observed in the product formed in the presence of $(NEt_4)(OAc)$ are nearly identical to carbonyl stretches of 2026 and 1958 cm^{-1} reported by Pickett and coworkers for a complex which contains similar donor atoms in the same geometry.[12] Metallation was also performed in the presence of the NEt_4^+ salt of the base 2,6-di-*tert*butyl-4-methoxyphenolate in order to avoid byproducts formed by binding of acetate to the iron center and to ensure deprotonation of the thiophenol moiety with a pK_a of approximately 7 (acetate conjugate acid pK_a ~5 vs. phenolate conjugate acid pK_a ~13). The isolated product was similar to that obtained using $(NEt_4)(OAc)$; however, the weak intensity of the carbonyl peaks obtained with both NEt_4^+ bases discouraged the possibility of isolating crystalline material suitable for diffraction.

Metallation was then performed using Hünig's base (NEt^iPr_2), a neutral, non-nucleophilic amine base. Treatment of **22** with Hünig's base at room temperature resulted in no significant color change over the course of 30 minutes. The salt $[Fe(CO)_4Br_2]$ was added at –40 °C and the reaction was monitored by solution IR spectroscopy. After stirring at cold temperature, warming to room temperature and continued stirring for one hour, the product exhibited three carbonyl stretches at 2073, 2015, and 1954 cm^{-1}. After continued stirring, the tricarbonyl species persisted, prompting the removal of solvent to purify and isolate the product. Treatment of the product with THF resulted in the loss of the carbonyl stretch at 2072 cm^{-1} and a small red-shift of the remaining two carbonyls to

2011 and 1950 cm^{-1}. The product exhibits good stability in the solid-state and in solution under dinitrogen atmosphere without appreciable loss of carbonyl intensity over the course of one month. Exposure to air or moisture, however, rapidly (t < 5 min) results in a color change to green, presumably decomposing the product to a high-spin Fe^{2+} species upon loss of carbonyls. Despite the favorable stability of the complex, crystallization attempts have not been successful with organic or inorganic counterions accounting for the expected charge of the product.

Scheme 8: Schematic representation of predicted dicarbonyl complexes possible resulting from metallation[a] of **22** with Hünig's base.

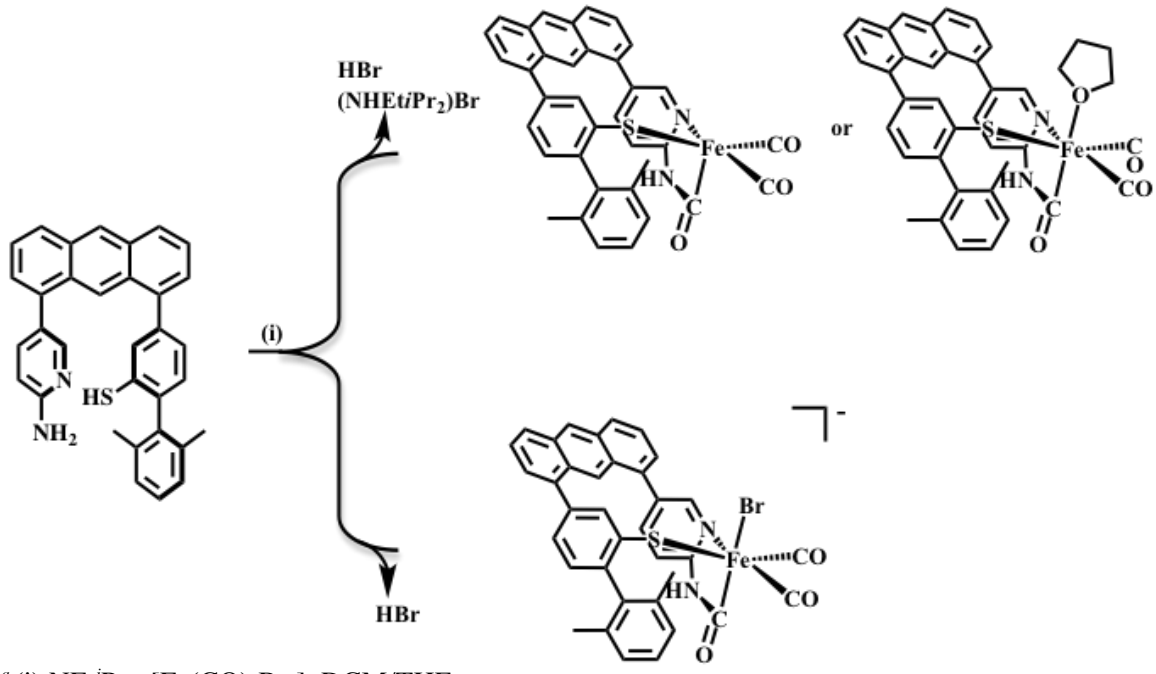

[a] (i) NEt^iPr_2, $[Fe(CO)_4Br_2]$, DCM/THF

The presence and identity of a base in the metallation of **22** with $[Fe(CO)_4Br_2]$ noticeably mediates the reactivity, resulting in the initial isolation of either a dicarbonyl or tricarbonyl species. The use of a charged, basic oxygen NEt_4^+ salt (i.e. acetate or phenolate) categorically resulted in a dicarbonyl species, presumably with generation of

the conjugate acid, loss of HBr, and the formation of the NEt_4^+ salt of the complex. In contrast, the use of neutral Hünig's base results in a tricarbonyl species, in which the other donor atoms could be some combination of S, C, N, or Br. Reaction between the ligand and anionic bases appears fast, evidenced by a rapid color change in solution from yellow to orange, while no color change is observed in the presence of Hünig's base. The use of Hünig's base may mediate slow deprotontation of the thiophenol moiety through a [S•••H•••N] hydrogen bonding interaction that decreases the nucleophilicity of the sulfur atom, prompting controlled binding to the metal center and preservation of the carbonyl ligands. Addition of THF to the tricarbonyl species results in conversion to a dicarbonyl species over the course of 24 hours; however, it is unclear if THF simply displaces a carbonyl ligand, binds to the complex, or enables binding of another ligand in this process (Scheme 8). It is notable that during this conversion the frequencies of the low energy carbonyls do not shift significantly upon conversion from the tricarbonyl to the dicarbonyl product. In contrast, during conversion of **7a** to the tricarbonyl analog, Hu and coworkers observed a significant shift in frequencies from 2022 and 1959 cm^{-1} in the dicarbonyl to 2073, 2024, and 1995 cm^{-1} in the tricarbonyl. This difference may be explained by the rigid structure imposed by the anthracene backbone, minimizing structural rearrangements that may occur in the other system.

In conclusion, the synthetic rationale and procedure for an anthracene-based ligand architecture for the development of synthetic models of mono [Fe]-hydrogenase have been described. Metallation of the ligand framework has been successfully performed; however, further structural characterization via X-ray crystallography or Extended X-ray Absorption Fine Structure (EXAFS) is necessary to elucidate the identity of the isolated dicarbonyl species. In the future, other ligands, such as phosphines, may be introduced in order to promote crystallization of a derivative species. Upon structural

characterization, studies will be performed to examine reactivity with dihydrogen and hydride transfer to organic substrates of relevance to mono [Fe]-hydrogenase. The reactivity will be analyzed and referenced to related complexes, namely **17** and **18**, in order to better understand the role of the anionic thiolate moiety in the enzyme active site and its relationship to catalysis. Furthermore, the thermodynamic hydricity of the complex will be calculated for comparison to other iron and precious metal hydrogenation catalysts and for methodical application of the complex in reactions of industrial relevance.

III. Materials and Methods

Reagents and General Procedures

Dry solvents were purified using a two-column alumina purification system (Pure Process Technology). Deuterated solvents were purchased from Cambridge Isotope Laboratories and used without further purification; the standard freeze–pump–thaw technique was used to degas deuterated solvents as necessary. The starting materials $[Pd_2(dba)_3]$ (Strem), XPhos and SPhos (Oakwood), and *tert*-nonyl mercaptan (Sigma) were purchased and used without further purification. The synthons 1,8-dichloroanthracene,[37] $[Fe(CO)_4Br_2]$,[12] were synthesized and purified according to previously reported procedures.

Synthesis of Ligand and Precursors

4-Bromo-2-(methylthio)aniline. An aqueous solution (600 mL) of KOH (84.0 g, 1.50 mol) and 2-amino-6-bromobenzothiazole (10.0 g, 43.6 mmol) was refluxed overnight. The solution was cooled to room temperature and iodomethane (6.23 g, 43.9 mmol) was added dropwise and stirred. The product was extracted in diethyl ether, dried over Na_2SO_4, and concentrated to afford a brown oil. Yield: 8.47 g (89%). ^{1}H NMR (400 MHz, $CDCl_3$): δ 7.43 (1H, d), 7.16 (1H, q), 6.59 (1H, d), 4.23 (2H, br s), 2.37 (3H, s). ^{13}C NMR (100 MHz, $CDCl_3$): δ 17.52, 109.61, 116.16, 122.38, 131.25, 134.66, 145.76. IR (neat, cm^{-1}): 3446, 3351, 2929, 1602, 1472, 807, 752. HRMS (ESI^+) *m/z:* $[M+H]^+$ calcd. for C_7H_8BrNS 217.96340; found 217.96330.

(5-Bromo-2-iodophenyl)(methyl)sulfane. The starting material 4-bromo-2-(methylthio)aniline (2.52 g, 11.5 mmol) was dissolved in acetone (10 mL) and cooled to 0 °C. Concentrated HCl (2.40 mL, 28.8 mmol) was added dropwise at 0 °C. The solution was cooled to –40 °C and an aqueous solution (4 mL) of NaNO2 (0.917 g, 13.5 mmol) was slowly added to the purple-brown solution to afford a bright yellow color. An aqueous solution (4 mL) of NaI (3.44 g, 23.7 mmol) was added at –40 °C and allowed to warm to room temperature, evolving N_2 gas as the reaction proceeded. The deep red solution was then extracted with DCM, washed with a solution of $Na_2S_2O_3$, and dried over Na_2SO_4. The product was purified by column chromatography in hexanes:EtOAc (20:1) and concentrated to a white crystalline solid. Yield: 3.00 g (79%). ^{1}H NMR (400 MHz, $CDCl_3$): δ 7.61 (1H, d), 7.15 (1H, d), 7.47 (1H, q), 2.48 (3H, s). ^{13}C NMR (100 MHz, $CDCl_3$): δ 16.97, 94.65, 123.10, 127.10, 128.83, 140.26, 145.61. IR (solid-state, cm^{-1}): 2963, 2912, 1551, 1422, 999, 843, 796. HRMS (CI^+) *m/z:* $[M+H]^+$ calcd. for C_7H_8BrINS 327.8418; found 327.8418.

(4-Bromo-2',6'-dimethyl-[1,1'-biphenyl]-2-yl)(methyl)sulfane. Under a dinitrogen atmosphere, a Schlenk flask was prepared with (5-bromo-2-iodophenyl)(methyl)sulfane (2.00 g, 6.08 mmol), $Ba(OH)_2$•$8H_2O$ (5.75 g, 18.2 mmol), 2,6-dimethylphenylboronic acid (1.00 g, 6.67 mmol), and 5% $[Pd(PPh_3)_4]$ (0.357 g, 0.304 mmol) in a degassed solution (160 mL) of 3:1 dioxane:H_2O. The solution was heated at 80 °C overnight. The solution was cooled to room temperature, extracted with DCM, and dried over Na_2SO_4. The product was purified by column chromatography in hexanes:EtOAc (20:1), and concentrated to a colorless solid. Yield: 1.64 g (88%). ^{1}H NMR (400 MHz, $CDCl_3$): δ 7.32 (2H, m), 7.21 (1H, q), 7.11 (2H, d), 6.89 (1H, q), 2.36 (3H, s), 1.98 (6H, s). ^{13}C NMR (100 MHz, $CDCl_3$): δ 14.79, 20.09, 121.67, 126.21, 127.35, 127.56, 127.97,

130.45, 136.41, 137.46, 138.09, 140.43. IR (solid-state, cm^{-1}): 2917, 1572, 1426, 1075, 999, 813, 744. HRMS (CI^+) *m/z:* $[M+H]^+$ calcd. for $C_{15}H_{15}BrS$ 306.0078; found 306.0081.

5-(8-Chloroanthracen-1-yl)pyridin-2-amine. Under a dinitrogen atmosphere, a Schlenk flask was prepared with 2-amino-5-bromopyridine (2.02 g, 11.6 mmol), potassium acetate (3.43 g, 35.0 mmol), bis(pinacolato)diboron (B_2Pin_2) (3.25 g, 12.8 mmol) and 3% by mol $Pd_2(dba)_3$ (0.301 g, 0.329 mmol) with SPhos (0.1488 g, 0.362 mmol) in dry dioxane (100 mL). The solution was refluxed for six hours. Degassed solutions of K_3PO_4 (7.38 g, 34.8 mmol) in H_2O (15 mL) and 1,8-dichloroanthracene (3.26 g, 13.2 mmol) in dioxane (20 mL) were added to the flask under a constant stream of dinitrogen. The resulting solution was refluxed overnight. The cooled solution was filtered over Celite, concentrated in vacuo, and column purified by gradient elution of hexanes:EtOAc (7:1 to 1:1). The product was isolated as a yellow-orange powder. Yield: 1.35 g (38%). ^1H NMR (400 MHz, $CDCl_3$): δ 8.90 (1H, s), 8.49 (1H, s), 8.31 (1H, m), 8.01 (1H, d), 7.93 (1H, d), 7.74 (1H, dd), 7.54 (2H, m), 7.39 (2H, m), 6.71 (1H, dd), 4.71 (2H, s). ^{13}C NMR (100 MHz, $CDCl_3$): δ 121.87, 125.15, 125.40, 125.81, 127.74, 129.03, 132.41, 139.61. IR (solid-state, cm^{-1}): 3398, 3344, 2973, 1639, 1506, 1370, 1102, 947, 741. HRMS (ESI^+) *m/z:* $[M+H]^+$ calcd. for $C_{19}H_{13}ClN_2$ 305.08400; found 305.08500.

5-(8-(2',6'-Dimethyl-2-(methylthio)-[1,1'-biphenyl]-4-yl)anthracen-1-yl)pyridin-2-amine. Under a dinitrogen atmosphere, a Schlenk flask was prepared with (4-bromo-2',6'-dimethyl-[1,1'-biphenyl]-2-yl)(methyl)sulfane (0.508 g, 1.65 mmol), potassium acetate (0.480 g, 4.89 mmol), bis(pinacolato)diboron (B_2Pin_2) (1.04 g, 4.07 mmol) and 5% by mol $Pd_2(dba)3$ (0.0986 g, 0.108 mmol) with XPhos (0.159 g, 0.333 mmol) in dry dioxane (50 mL). The solution was refluxed overnight, affording a dark brown solution.

Degassed solutions of K_3PO_4 (1.04 g, 4.91 mmol) in H_2O (10 mL) and 5-(8-chloroanthracen-1-yl)pyridin-2-amine (0.548 g, 1.80 mmol) in dioxane (20 mL) were added to the flask under a constant stream of dinitrogen. The resulting brown-orange solution was refluxed overnight. The cooled solution was filtered over Celite, concentrated in vacuo, and column purified in a gradient elution of hexanes:EtOAc (7:1 to 1:1). The product was isolated as a yellow powder. Yield: 0.665 g (81%). ^{1}H NMR (400 MHz, $CDCl_3$): δ 8.67 (1H, s), 8.57 (1H, s), 8.15 (1H, s), 8.05 (2H, t), 7.56 (5H, m), 7.36 (1H, dd), 7.33 (1H, s), 7.31 (1H, d), 7.18 (1H, m), 7.16 (1H, m) 7.11 (1H, dd), 6.52 (1H, d), 4.67 (2H, br s), 2.26 (3H, s), 2.08 (6H, s). IR (solid-state, cm^{-1}): 3419, 2978, 1614, 1260, 1107, 948, 883, 746. HRMS (ESI^+) *m/z:* $[M+H]^+$ calcd. for $C_{35}H_{29}N_2S$ 496.20930; found 496.21000.

4-(8-(6-Aminopyridin-3-yl)anthracen-1-yl)-2',6'-dimethyl-[1,1'-biphenyl]-2-thiol. Under inert atmosphere, sodium hydride (0.126 g, 5.24 mmol) was suspended in DMF (3 mL). *Tert*-nonylmercaptan (0.843 g, 5.25 mmol) was added dropwise to the solution of sodium hydride forming a colorless solution following the evolution of H_2 gas. A DMF solution (3 mL) of 5-(8-(2',6'-dimethyl-2-(methylthio)-[1,1'-biphenyl]-4-yl)anthracen-1-yl)pyridin-2-amine (0.653 g, 1.31 mmol) was added to the flask and the resulting red-orange solution was refluxed overnight under dinitrogen. The solution was cooled and the product was precipitated by addition to a solution (100 mL) of 3 M HCl. The product was collected by vacuum filtration and washed with water, before drying under high vacuum. The product was isolated as a yellow powder. Yield: 0.292 g (46%). ^{1}H NMR (400 MHz, $CDCl_3$): 8.67 (1H, s), 8.56 (1H, s), 8.15 (1H, s), 8.05 (2H, t), 7.55 (5H, m), 7.53 (1H, d), 7.48 (1H, s), 7.37 (1H, d), 7.34(1H, d), 7.21 (1H, s) 7.19 (1H, dd), 6.61 (1H, d), 4.67 (2H,

br s), 2.09 (6H, s). IR (solid-state, cm^{-1}): 2959, 2562, 1683, 1583, 1261, 1096, 874, 744. HRMS (CI^+) *m/z:* $[M+H]^+$ calcd. for $C_{33}H_{25}N_2S$ 482.1817; found 482.1811.

SYNTHESIS OF METAL COMPLEXES

Metallation without base. Under a dinitrogen atmosphere, the ligand **22** (0.100 g, 0.207 mmol) was dissolved in 5 mL dry dichloromethane (CH_2Cl_2). The solution was cooled to –40 °C and a CH_2Cl_2 solution (5 mL) of $[Fe(CO)_4Br_2]$ (0.0679 g, 0.207 mmol) was added dropwise to afford a deep red colored solution. The reaction was stirred at –40 °C for 15 minutes and then warmed to room temperature. The solution was concentrated in vacuo and precipitated from Et_2O to afford a yellow-orange powder. IR *v*(CO) (solid-state, cm^{-1}): 2096, 2040, 1613.

General Procedure for NEt_4^+ bases. Under a dinitrogen atmosphere, the ligand **22** (0.100 g, 0.207 mmol) was dissolved in 5 mL dry dichloromethane (CH_2Cl_2). An equivalent of base ($(NEt_4)(OAc)$ or (NEt_4)(2,6-di-*tert*butyl-4-methoxyphenolate)) (0.207 mmol) dissolved in CH_2Cl_2 (3 mL) was added to the ligand solution, resulting in an immediate color change from yellow to orange. The solution was cooled to –40 °C and a CH_2Cl_2 solution (5 mL) of $[Fe(CO)_4Br_2]$ (0.0679 g, 0.207 mmol) was added dropwise to afford a deep red colored solution. The reaction was stirred at –40 °C for 15 minutes and then warmed to room temperature. The solution was concentrated in vacuo and purified by a pipette column packed with neutral alumina, eluting with CH_2Cl_2. The product was concentrated to a yellow-orange powder. IR *v*(CO) (solid-state, cm^{-1}): 2025, 1962, 1613.

Metallation with Hünig's base. Under a dinitrogen atmosphere, the ligand **22** (0.100 g, 0.207 mmol) was dissolved in 5 mL dry dichloromethane (CH_2Cl_2). A small excess of Hünig's base (NEt^iPr_2) (43.3 μL, 0.249 mmol) was added by microsyringe to the ligand

solution and stirred at room temperature for 30 minutes with no significant change in the yellow colored solution. The solution was cooled to –40 °C and CH_2Cl_2 solution (5 mL) of [$Fe(CO)_4Br_2$] (0.0679 g, 0.207 mmol) was added dropwise to afford a deep red colored solution. The reaction was stirred at –40 °C for one hour and then warmed to room temperature. The solution was concentrated in vacuo, then redissolved in tetrahydrofuran (10 mL) and stirred overnight in the dark at room temperature. The resulting orange solution was first Celite-filtered to separate it from a dark colored precipitate, then concentrated and washed with Et_2O to afford an orange powder. IR *v*(CO) (solid-state, cm^{-1}): 2011, 1950, 1632.

Ion Exchange. Under a dinitrogen atmosphere, the complex (0.0753 g, 0.0904 mmol) was dissolved in THF (10 mL) and stirred with an excess (0.146 g, 0.452 mmmol) of the 15-crown-5 salt of NaBr. The orange solution was stirred for one hour, affording a turbid orange solution with [NHEt*i*Pr_2]Br as the expected precipitate. The solution was filtered through celite and concentrated in vacuo to afford a sticky, dark orange solid. The product was washed with Et_2O to remove the excess of the crown salt and residual THF to afford an orange powder.

PHYSICAL MEASUREMENTS

The ^1H and ^{13}C NMR spectra were obtained on a Varian DirectDrive spectrometer (400 MHz), with reported chemical shifts (δ, ppm) referenced to the respective solvents. IR spectra were collected on a Bruker Alpha Fourier transform infrared (FTIR) spectrometer equipped with a diamond ATR crystal. Mass spectrometry (MS) data were collected on an Agilent Technologies 6530 Accurate Mass Q-Tof LC/MS (ESI) or Micromass Autospec Ultima (CI).

IV. SPECTROSCOPIC DATA

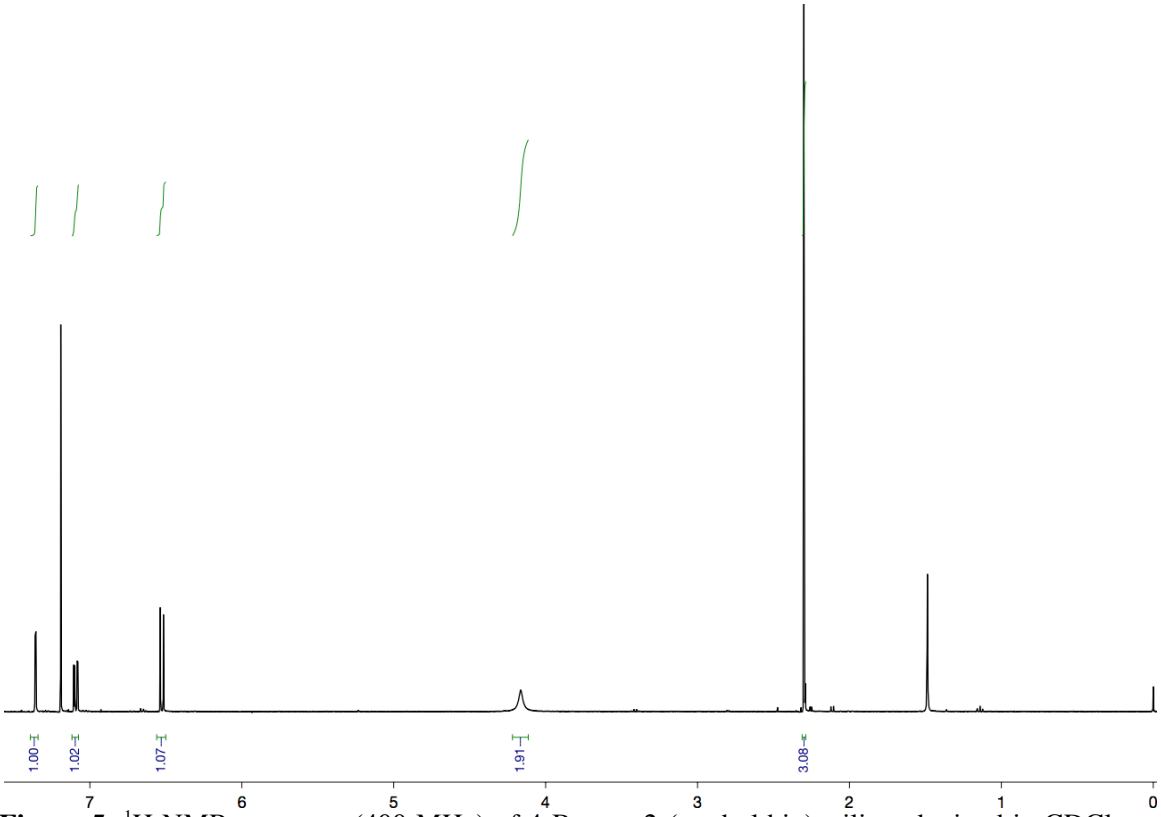

Figure 5: ^{1}H NMR spectrum (400 MHz) of 4-Bromo-2-(methylthio)aniline obtained in $CDCl_3$ at 25 °C.

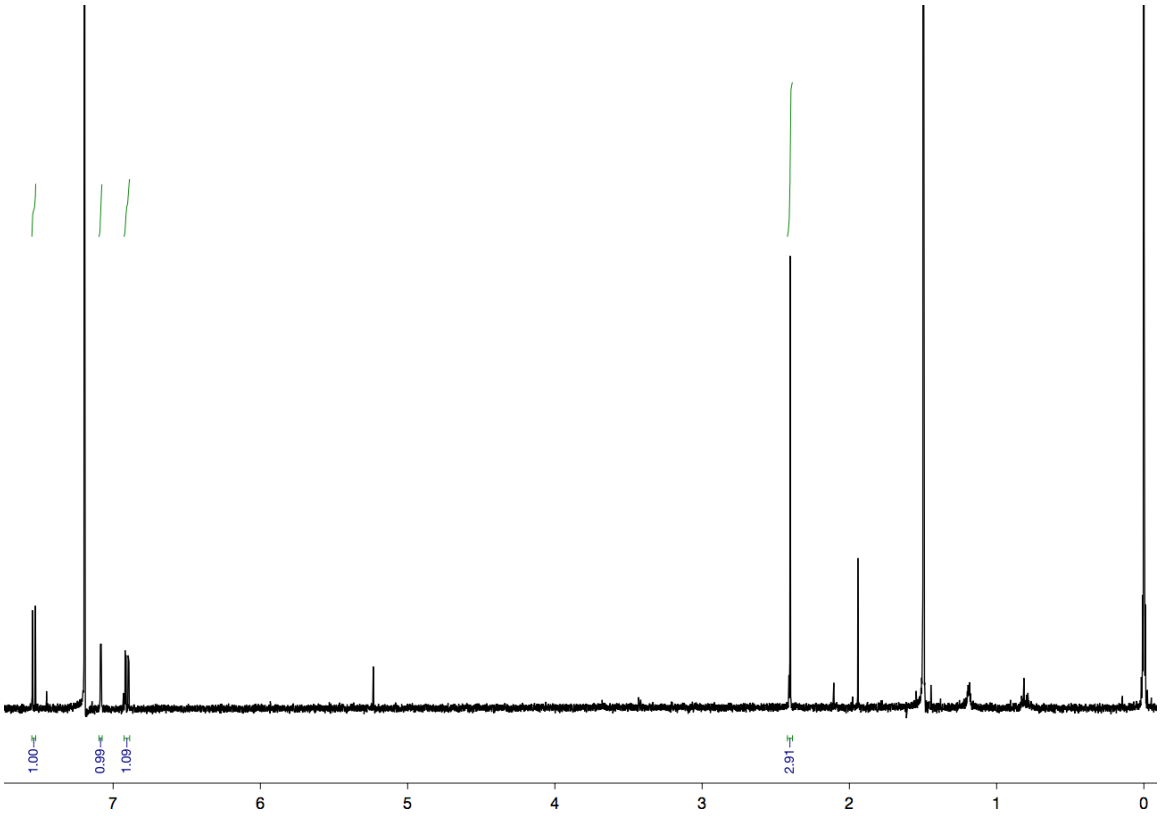

Figure 6: ^{1}H NMR spectrum (400 MHz) of (5-Bromo-2-iodophenyl)(methyl)sulfane obtained in $CDCl_3$ at 25 °C.

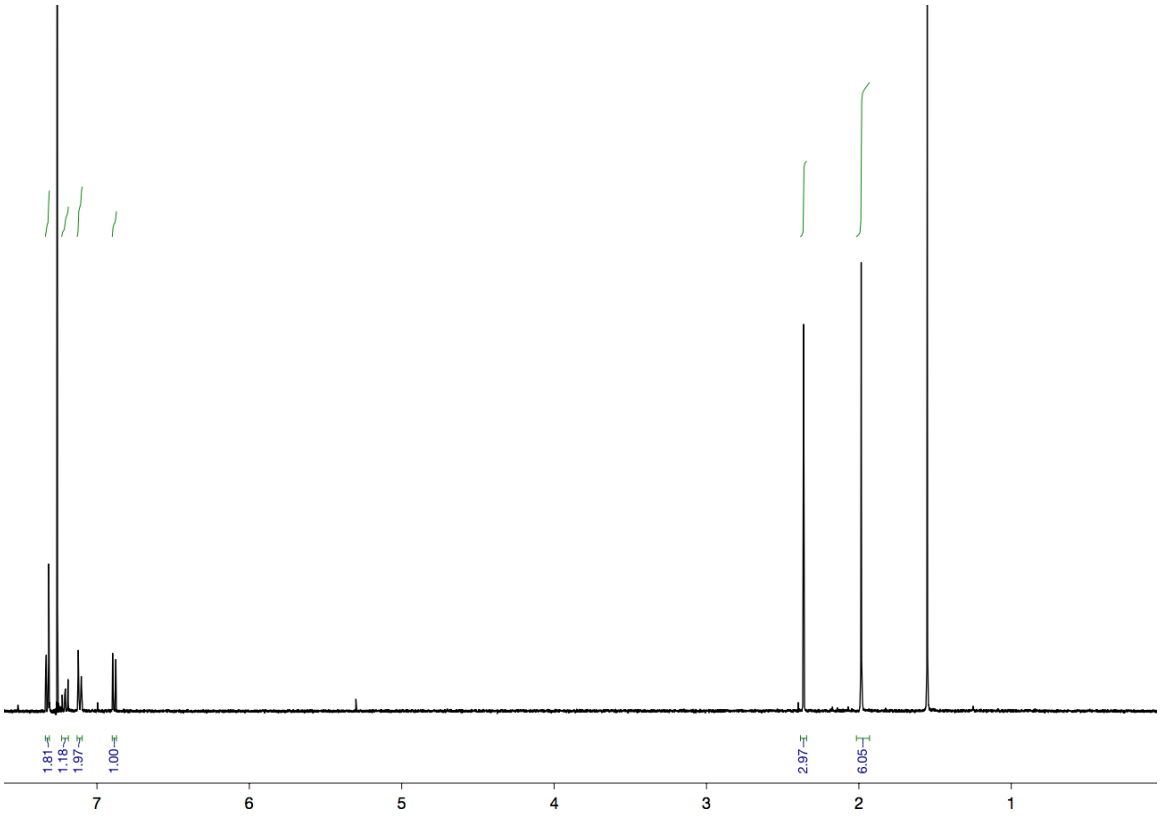

Figure 7: ^{1}H NMR spectrum (400 MHz) of (4-Bromo-2',6'-dimethyl-[1,1'-biphenyl]-2-yl)(methyl)sulfane obtained in $CDCl_3$ at 25 °C.

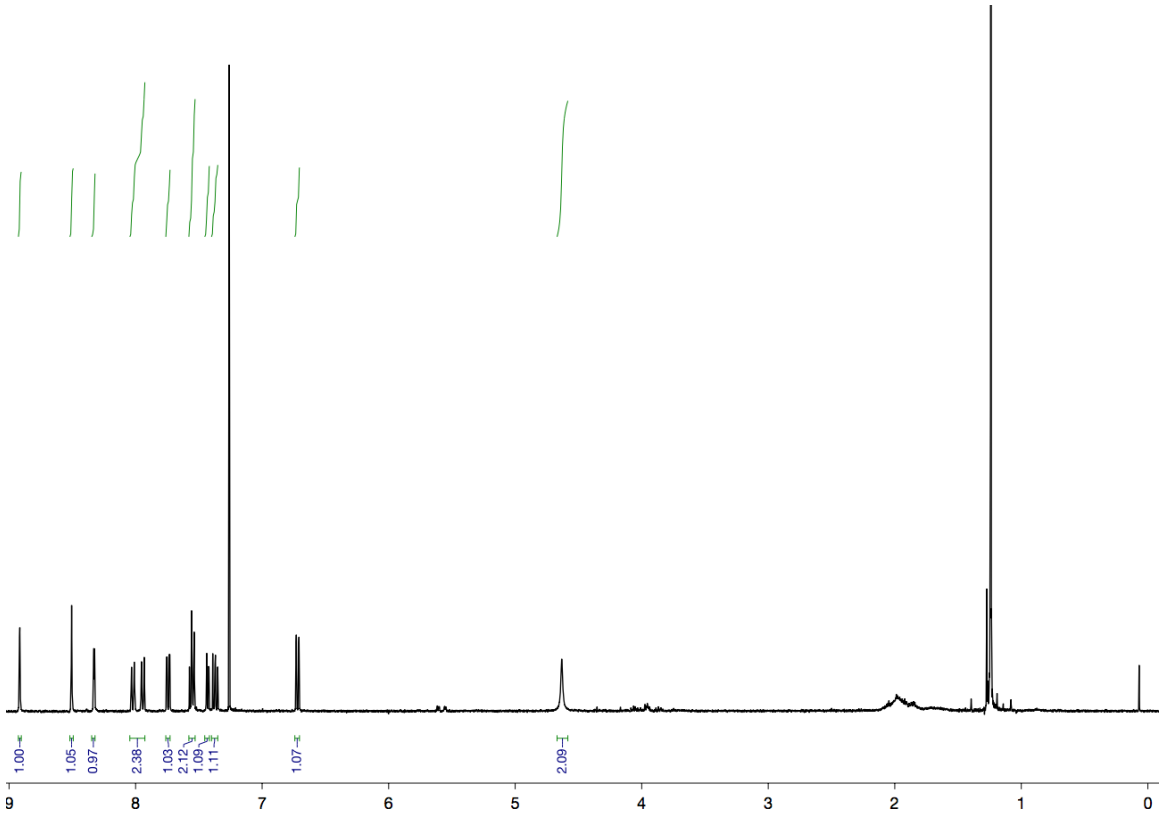

Figure 8: ^{1}H NMR spectrum (400 MHz) of 5-(8-Chloroanthracen-1-yl)pyridin-2-amine obtained in $CDCl_3$ at 25 °C.

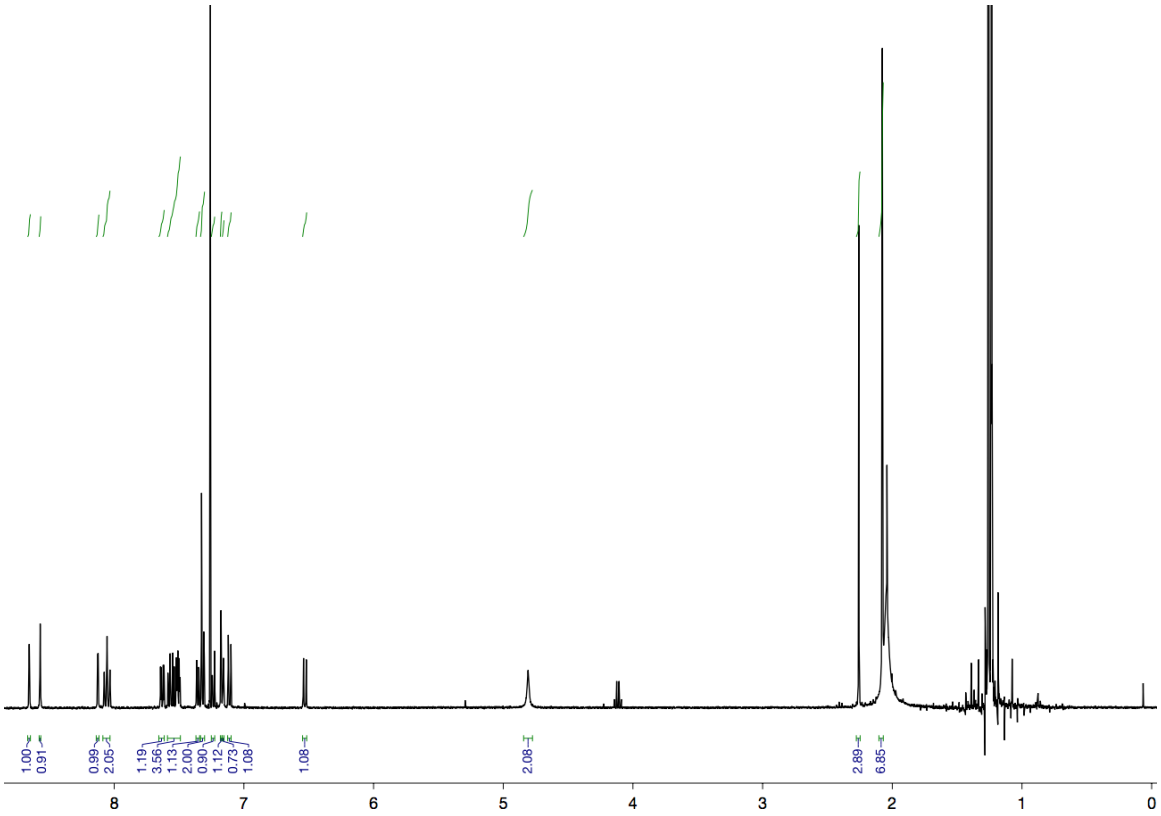

Figure 9: ^{1}H NMR spectrum (400 MHz) of 5-(8-(2',6'-Dimethyl-2-(methylthio)-[1,1'-biphenyl]-4-yl)anthracen-1-yl)pyridin-2-amine obtained in $CDCl_3$ at 25 °C.

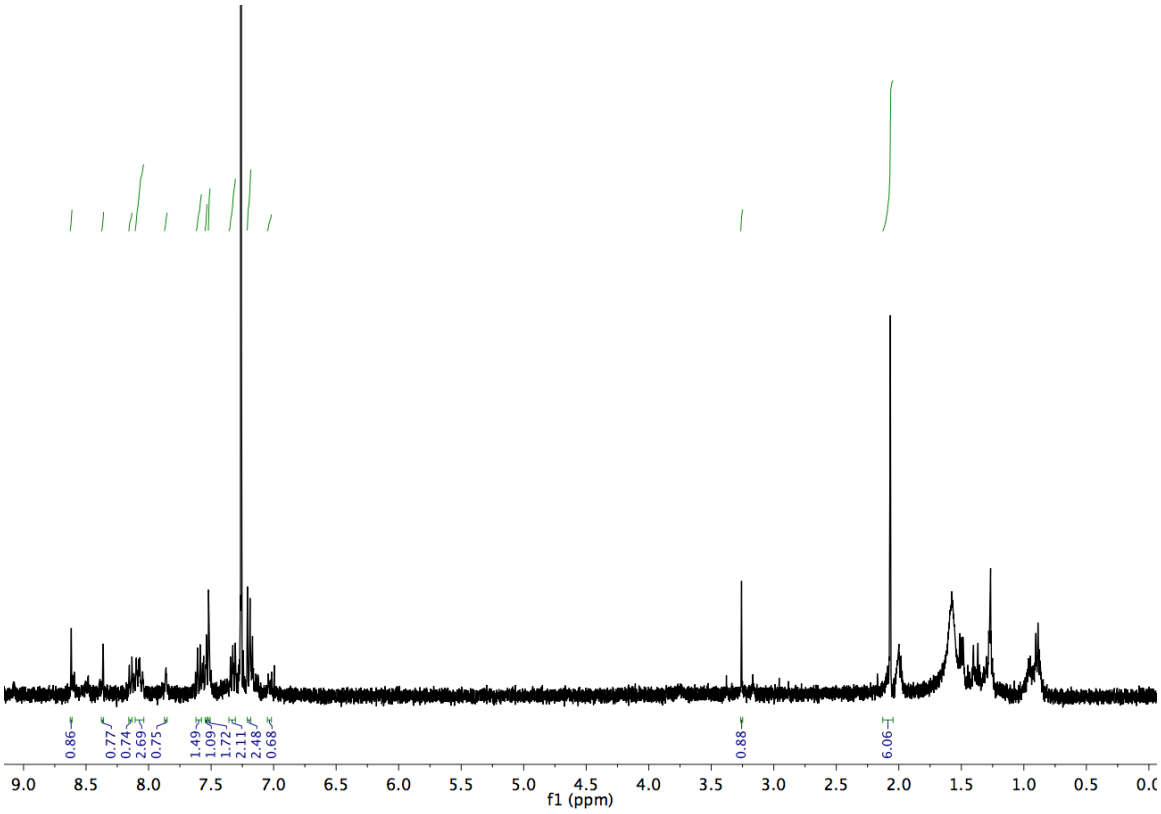

Figure 10: ^{1}H NMR spectrum (400 MHz) of 4-(8-(6-Aminopyridin-3-yl)anthracen-1-yl)-2',6'-dimethyl-[1,1'-biphenyl]-2-thiol obtained in $CDCl_3$ at 25 °C.

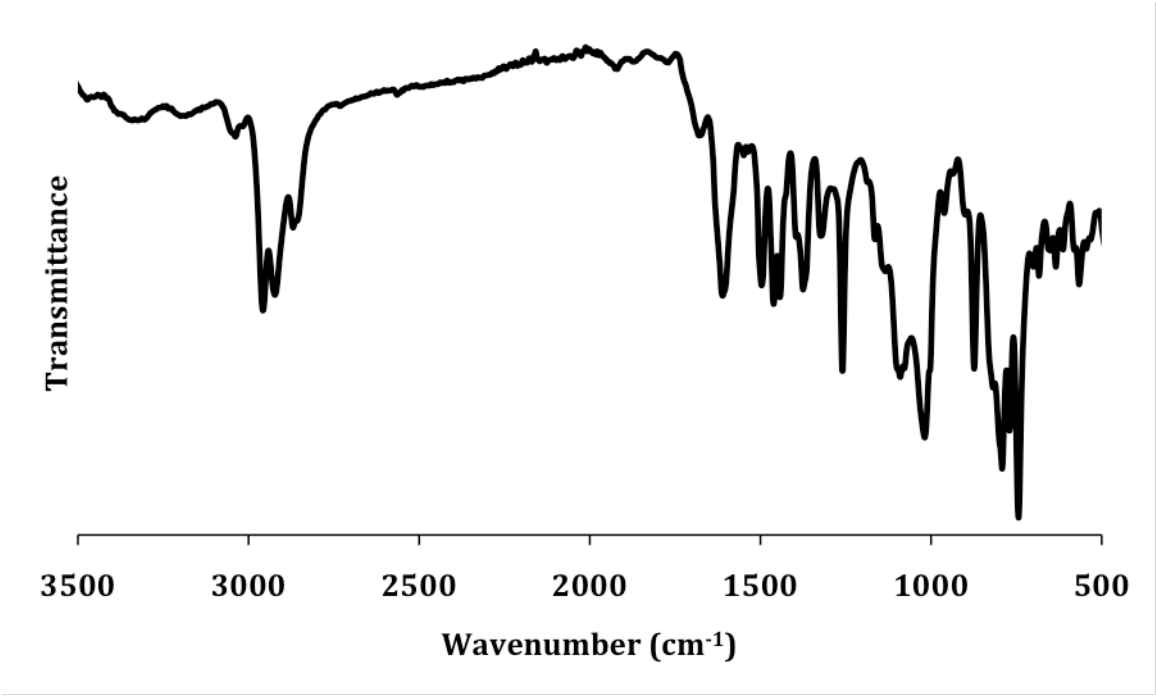

Figure 11: Solid-state IR spectrum of 4-(8-(6-Aminopyridin-3-yl)anthracen-1-yl)-2',6'-dimethyl-[1,1'-biphenyl]-2-thiol (298 K, ATR crystal).

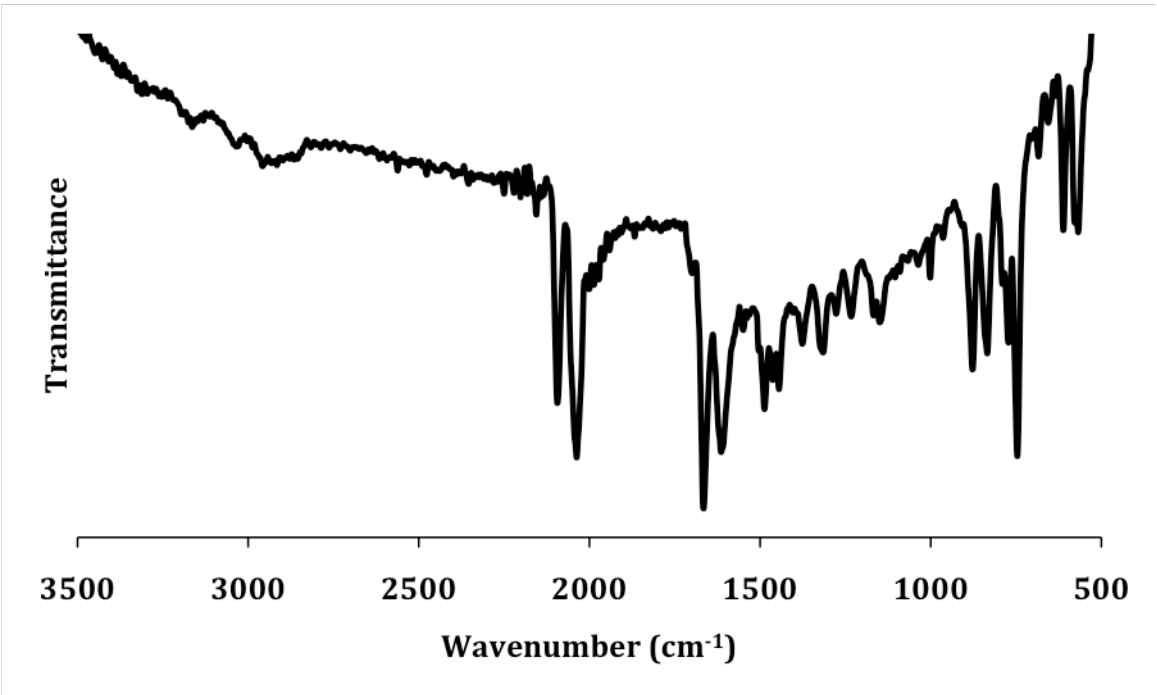

Figure 12: Solid-state IR spectrum of iron dicarbonyl species obtained in the absence of base (298 K, ATR crystal).

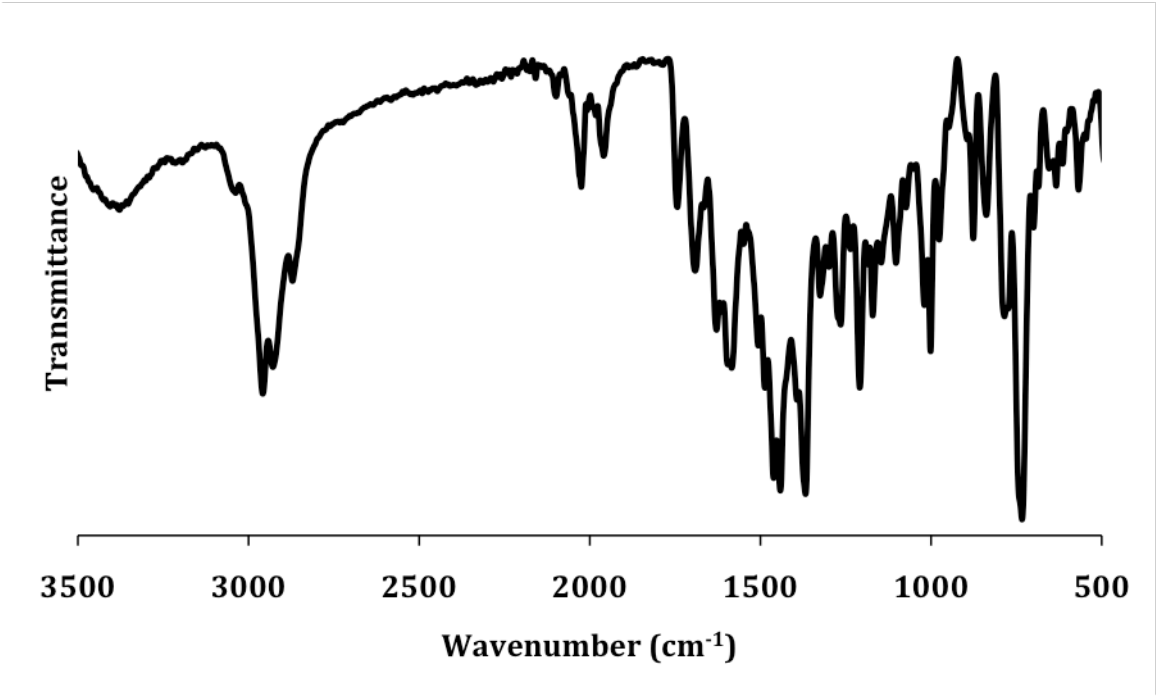

Figure 13: Solid-state IR spectrum of iron dicarbonyl species obtained using NEt_4^+ bases (298 K, ATR crystal).

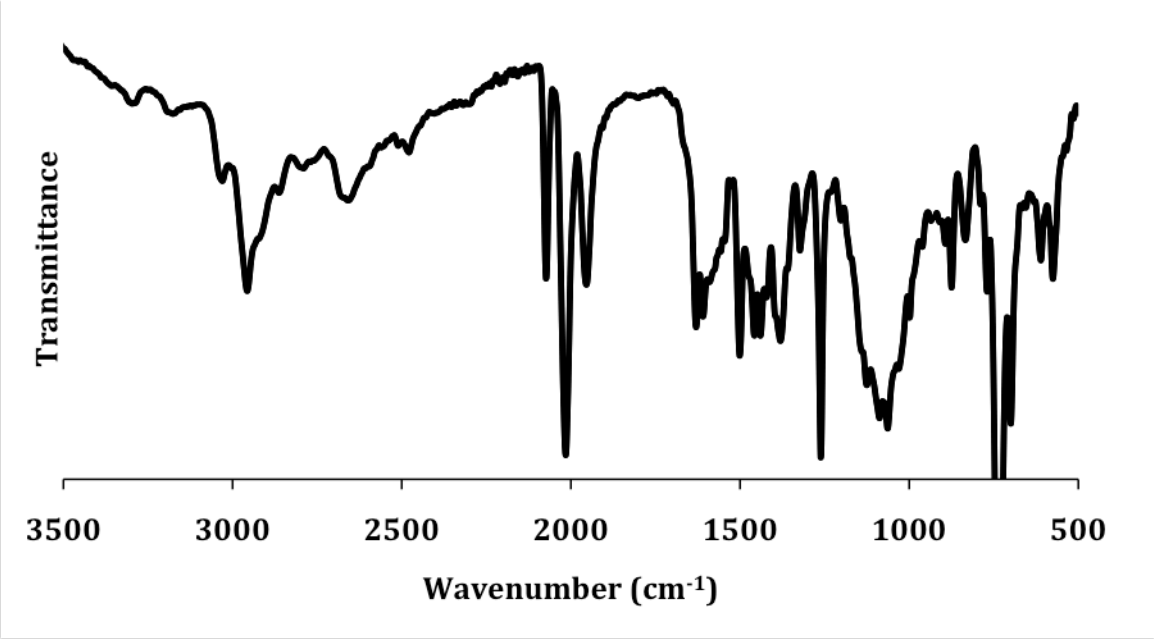

Figure 14: Solid-state IR spectrum of iron tricarbonyl species obtained using Hünig's base (298 K, ATR crystal).

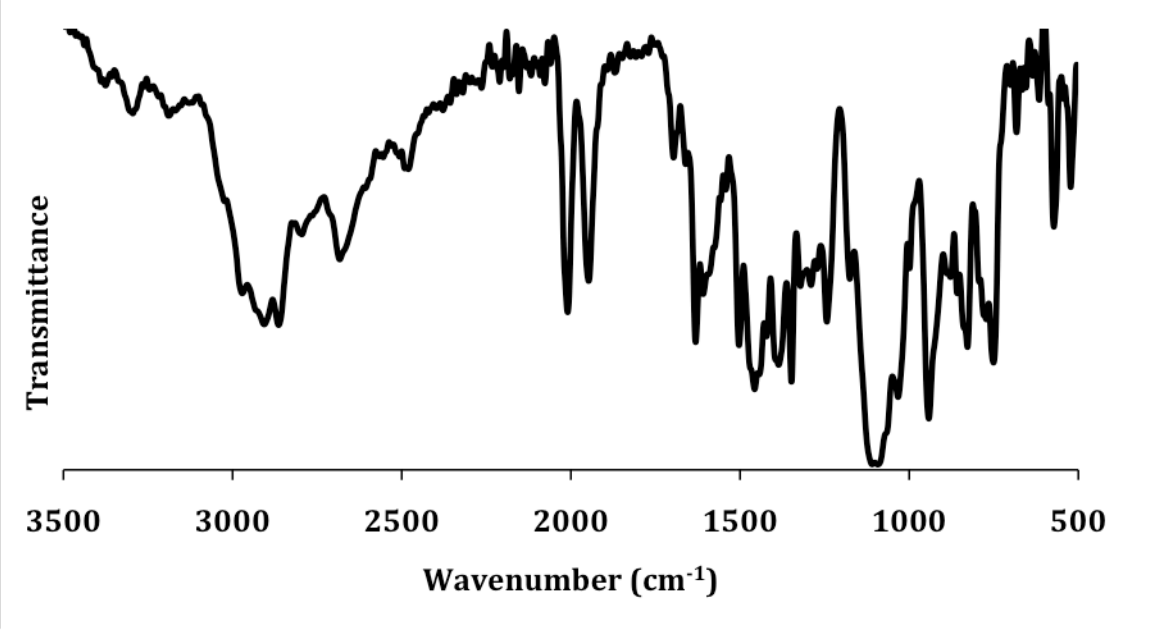

Figure 15: Solid-state IR spectrum of iron dicarbonyl species obtained following treatment of tricarbonyl species with THF and ion exchange (298 K, ATR crystal).

V. REFERENCES

1. (a) Volbeda, A.; Garcin, E.; Piras, C.; Fernandez, V. M.; Hatchikian, E. C.; Frey, M.; Fontecilla-Camps, J. C. *J. Am. Chem. Soc.* **1996**, *118,* 12989. (b) Pandey, A. S.; Harris, T. V.; Giles, L. J.; Peters, J. W. Szilagyi, R. K. *J. Am. Chem. Soc.* **2008**, *130*, 4533. (c) Fujishiro, T.; Ataka, K.' Ermler, U.; Shima, S. *FEBS Journal* **2015**, *282*, 3412.
2. Lyon, E. J. ; Shima, S.; Buurman, G.; Shantanu, C.; Batschauer, A.; Steinbach, K.; Thauer, R.K. *Eur. J. Biochem.* **2004**, *271*, 195.
3. Lyon, E.J.; Shima, S.; Boecher, R.; Thauer, R.K.; Grevels, F.W.; Bill, E.; Roseboom,W.; Albracht, S. P. J. *J. Am. Chem. Soc.* **2004**, *126*, 14239.
4. Korbas, M.; Vogt, S.; Meyer-Klaucke, W.; Bill, E.; Lyon, E.J.; Thauer, R.K.; Shima, S. *J. Biol. Chem.* **2006**, *281*, 30804.
5. Shima, S.; Lyon, E. J.; Thauer, R. K.; Mienert, B; Bill, E. *J. Am. Chem. Soc.* 2005, 127, 10430.
6. Wang, X.F.; Li, Z. M.; Zeng, X. R.; Luo, Q.Y.; Evans, D. J.; Pickett, C. J.; Liu, X. M. *Chem. Commun.* **2008**, *45*, 3555.
7. Shima, S.; Pilak, O.; Vogt, S.; Schick, M.; Stagni, M. S.; Meyer-Klaucke, W.; Warkentin, E.; Thauer, R. K.; Ermler, U. *Science* **2008**, *321*, 572.
8. Hiromoto, T.; Ataka, K.; Pilak, O.; Vogt, S.; Stagni, M.S.; Meyer-Klaucke, W.; Warkentin, E.; Thauer, R. K.; Shima, S.; Ermler, U. *FEBS Letters* **2009**, *583*, 585.
9. Tard, C.; Pickett, C. J. *Chem. Rev.* **2009**, *109*, 2245.
10. Chen, D. F.; Scopelliti, R.; Hu, X. L. *J. Am. Chem. Soc.* **2010**, *132*, 928.
11. Chen, D. F.; Scopelliti, R.; Hu, X. L. Hu, *Angew. Chem. Int. Ed.* **2010,** *49*, 7512.

12. Turrell, P. J.; Wright, J. A.; Peck, J. N. T.; Oganesyan, V. S.; Pickett, C. J. *Angew. Chem. Intl. Ed.* **2010**, *49*, 7508.

13. Chen, D. F.; Scopelliti, R.; Hu, X. L. *Angew. Chem. Int. Ed.* **2011**, *50*, 5670.

14. Hu, B. W.; Chen, D. F.; R.; Hu, X. L. *Chem. Eur. J.* **2012**, *18*, 11528.

15. Hu, B. W.; Chen, D. F.; R.; Hu, X. L. *Chem. Eur. J.* **2014**, *20*, 1677.

16. Song, L.-C.; Xie, Z.-J.; Wang, M.-M.; Zhao, G.-Y.; Song, H.-B. *Inorg. Chem.* **2012**, *51*, 7466.

17. Song, L.-C.; Hu, F.-Q.; Zhao, G.-Y.; Zhang, J.-W.; Zhang, W.-W. *Organometallics* **2014**, *33*, 6614.

18. Kaganovsky, L.; Cho, K.; Gelman, D. *Organometallics* **2008**, *27*, 5139–5145.

19. Bessel, C. A.; Aggarwal, P.; Marschilok, A. C.; Takeuchi, K. J. *Chem. Rev.* **2001**, *101*, 1031.

20. Elsevier, C. J.; Reedijk, J.; Walton, P. H.; Ward, M. D. *Dalton Trans.* **2003**, 1869.

21. Lee, C.-L.; Chisholm, J.; James, B.; Nelson, P. A.; Lilga, M. A. *Inorg. Chim. Acta* **1986**, *121*, L7.

22. Jessop, P. G.; Rettig, S. J.; Lee, C.-L.; James, B. R., *Inorg. Chem.* **1991**, *30*, 4617.

23. Liaw, W.-F.; Kim, C.; Darensbourg, M. Y.; Rheingold, A. L. *J. Am. Chem. Soc.* **1989**, *111*, 3591.

24. Darensbourg, M.Y.; Liaw, W.-F.;Riordan, C. G. *J. Am. Chem. Soc.* **1989**, *111*, 8051.

25. Wander, S. A.; Reibenspies, J. H.; Kim, J.-S.; Darensbourg, M. Y. *Inorg. Chem.* **1994**, *33*, 1421.

26. Khasnis, D. V.; Pirio, N.; Touchard, D.; Toupet, L.; Dixneuf, P. H. *Inorg. Chim. Acta* **1992**, *198*, 193.

27. Field, L. D.; Lawrenz, E. T.; Shaw, W. J.; Turner, P. *Inorg. Chem.* **2000**, *39*, 5632.

28. Field, L. D.; Shaw, W. J.; Turner, P. *Organometallics*. **2001**, *20*, 3491.

29. Field, L. D.; Shaw, W. J.; Turner, P. *Chem. Commun*. **2002**, 46.

30. Kimblin, C.; Churchill, D. G.; Bridgewater, B. M.; Girard, J. N.; Quarless, D. A.; Parkin, G. *Polyhedron*, **2001**, *20*, 1891.

31. Zheng, T.; Li, M.; Sun, H.; Harms, K.; Li, X. *Polyhedron*, **2009**, *28*, 3823.

32. Xue, B.; Sun, H.; Li. X. *RSC Adv*. **2015**, *5*, 52000.

33. Takaoka, A.; Mankad, N. P.; Peters, J. C. *J. Am. Chem. Soc*. **2011**, *133*, 8440

34. Yang, X.; Hall, M. B. *J. Am. Chem. Soc*. **2009**, *131*, 10901.

35. Ogata, H.; Nishikawa, K.; Lubitz, W. *Nature* **2015**, *520*, 571.

36. Wiedner, E. S.; Chambers, M. B.; Pitman, C. L.; Bullock, R. M.; Miller, A. J. M.; Appel, A. M. *Chem. Rev*. **2016**, *116*, 8655.

37. Seo, J.; Ali, A. K.; Rose, M. J. *Comments Inorg. Chem*. **2014**, *34*, 103.

38. Manes, T.; Rose, M.J. *Inorg. Chem*. **2016**, *55*, 5127.